Elastocapillary Transition in Gel Drop Oscillations

X. Shao, S. A. Fredericks, J. R. Saylor, and J. B. Bostwick 1

¹Department of Mechanical Engineering, Clemson University, Clemson, South Carolina 29634, USA ²Department of Mechanical Engineering, University of Minnesota, Minneapolis, Minnesota 55455, USA

(Received 14 June 2019; published 31 October 2019)

We report experimental observations of surface oscillations in an ultrasoft agarose gel drop. Ultrasonic levitation is used to excite shape oscillations in the gel drop and we report the natural frequency of the drop as it depends upon a nondimensional elastocapillary number, which we define as the ratio of the elastocapillary length to drop size. Our experiments span a wide range of experimental parameters and we recover the appropriate scaling laws in the elastic and capillary wave limits. The crossover between these two limits is observed and agrees well with a proposed frequency relationship.

DOI: 10.1103/PhysRevLett.123.188002

It has been known since the time of Lord Rayleigh (1879) [1] that a liquid drop will oscillate about its equilibrium shape reflecting a balance between inertia and capillarity, with the dynamics well established for Newtonian fluids [2–4]. In contrast, relatively little is known about the oscillations of gel drops despite its relevance to a number of emerging 3D printing technologies that utilize complex fluids in the printing process, such as the hydrogel-based bioinks used in tissue engineering [5,6] or the polymer-based functional inks for wearable electronics [7]. In this work, we perform drop oscillation experiments on agarose gels and characterize the competing effects of elasticity and surface tension on the drop natural frequency through observation of the crossover between capillary and elastic waves.

Gels are typically formed by polymerization and have been an important part of polymer science for some time [8]. Their importance has grown in recent years due to innovations in bioprinting technologies such as cell printing [9], which often use agarose or alginate gels because they are capable of sustaining biological function. Cell viability is often linked to the strains experienced by the cell within the gel drop and to print complex scaffold architectures requires the ability to precisely control the formation of drop surface patterns, both of which would benefit from a better understanding of the drop oscillation dynamics. Gels often have complex rheologies such that surface tension and elasticity are comparable, which prevents any simplification of our understanding of this necessarily multiphysics process.

Surface tension becomes important in gels on length scales where the surface energy is comparable to the elastic energy, as measured by the bulk elastocapillary length $\ell_e \equiv \sigma/G$, where σ is the surface tension and G the shear modulus of the material [10,11]. In common materials such as glass ($G \sim 10$ GPa) the elastocapillary length is smaller than the atomic scale $\ell_e < \text{Å}$, but in gels ($G \sim 10$ Pa) it is

macroscopic $\ell_e \sim 10^{-3}$ m. It is perhaps then unsurprising that many classical capillary driven instabilities in fluids have been observed in soft solids, such as the Rayleigh-Taylor [12,13] and Plateau-Rayleigh [14] instabilities, among many others [15-19]. On the other hand, from the fluid mechanical perspective, liquid elasticity affects dynamic wetting phenomena and can suppress splashing during drop deposition [20–22]. In our experiments, we use gels with $0.3 < \ell_e < 16$ mm such that our experiments with typical $R \sim \mathcal{O}(1)$ mm radius drops are able to capture the crossover between the elastic $\ell_e < R$ and capillary $\ell_e > R$ limits. [Note that our drops are smaller than the capillary length $R < l_c \equiv \sqrt{\sigma/\rho g}$ such that gravitational and elastogravity effects are negligible.] The elastocapillary crossover has been observed by Monroy and Langevin [23] for planar waves but to our knowledge has not been observed for free drops.

Ultrasonic levitation is used to realize a free drop in our experiments under terrestrial conditions [24–26], but magnetic [27] and aerodynamic [28–30] fields have also been used. This procedure eliminates wetting effects, which are known to affect the drop dynamics even in the case of inviscid liquids [31]. This is sometimes referred to as a containerless process. Shape oscillations can be excited in the drop by amplitude modulating the carrier wave field at a prescribed frequency. For an inviscid liquid drop, these are Rayleigh oscillations [1] and obey the following dispersion relationship

$$\omega_R^2 = \frac{n(n+2)(n-1)\sigma}{\rho R^3},\tag{1}$$

where ω is the angular frequency, ρ the density, and n the polar wave number. Of note is the fundamental n=2 mode which has the lowest nonzero frequency and undergoes oblate-prolate oscillations, as shown in Fig. 1. This technique

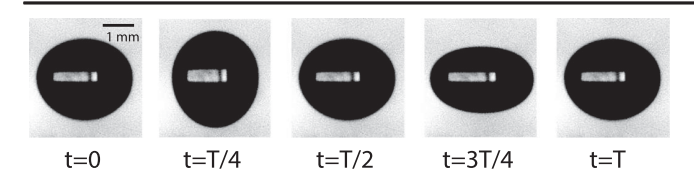


FIG. 1. Typical drop oscillation over a cycle of period T. Note the static drop (t=0) is slightly flattened (aspect ratio W/H=1.15) due to the acoustic pressure required to levitate the drop.

has been used to examine the role of viscosity [32] and surfactants [33] in liquid drops on Eq. (1), as well as explore the shape change dynamics of drops of aqueous foam [34] and blood [35]. To our knowledge there have been no extensions of Eq. (1) for free drops that include elasticity, which naturally must encompass the spheroidal modes for a linear elastic sphere [36–39]. However, Chakrabarti and Chaudhury [40] have notably documented the frequency response of sessile hydrogel drops. Our interest is in the elastocapillary transition for free drops.

Experiment.—In our experiments, we prepare gel drops using the density gradient method in order to ensure a spherical shape and eliminate evaporative effects [41]. An agarose solution is made by dissolving agarose powder (Sigma Aldrich Type VI-A) in doubly distilled water at 90 °C for 1 h at a desired concentration [42]. The range of concentrations investigated was $\phi = 0.077-0.285$ wt%, which are above the gel transition $\phi = 0.013$ [42]. The solution is injected into a liquid mixture of silicone oil (PDM-7040, Gelest) $\rho = 1.07$ g/mL and n-octane (Acros organics) $\rho = 0.7$ g/mL, whose density gradient spans that of the agarose solution $\rho = 1$ g/mL. The gel drop orients itself at the interface of the silicone oil/octane mixture and is allowed to gel (without evaporation) at room temperature for 3 h or more. The result is a highly spherical gel drop of known concentration. The range of sizes are R =1.16–1.63 mm. The drops are removed from the mixture and successively washed twice in n-heptane (Fisher Chemicals) for 2 min to remove any excess silicone oil or octane and then levitated for 15 sec to ensure the remaining heptane had evaporated. We measure the complex modulus G = G' + iG'' of each concentration using an Anton Paar rheometer (MCR 302). Here the loss modulus G'' is many orders of magnitude smaller than the storage modulus G' and our gels behave as linear elastic solids characterized by the shear modulus $G \equiv G'$, consistent with other studies of agarose gels [23,42,43]. The range of shear modulus investigated is G = 2.8-200.3 Pa. Because of the relatively dilute agarose concentrations used here, we assume the surface tension of the gel drop to be that of water $\sigma = 72$ mN/m.

The drop is levitated in an ultrasonic transducer, as shown schematically in Fig. 2, which consists of a horn and reflector separated by an integer number of half wavelengths [44]. The carrier wave is excited by the PZT

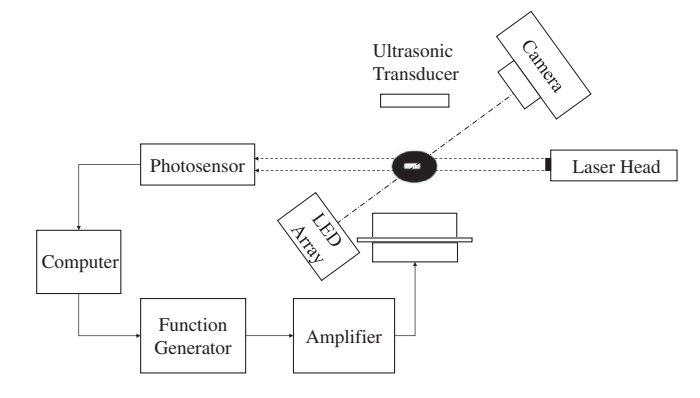


FIG. 2. Schematic of experimental setup illustrating the ultrasonic levitation technique.

transducer at 30.3 kHz and then amplitude modulated (AM) over a range of frequencies near the drop resonance. The AM frequency sweep excites oblate-prolate shape oscillations in the drop, as shown in Fig. 1. These correspond to the n=2 mode in Eq. (1). The frequency sweep typically takes 3 min over which time evaporation is minimal. It is worth noting that the acoustic pressure required to levitate the drop also tends to flatten it (statically) such that the width W to height H ratio deviates from sphericity W/H = 1 (cf. Fig. 1 t = 0). That ratio in our experiments is W/H = 1.167-1.432, the sphericity of the drops outside of the acoustic field notwithstanding.

The magnitude of the drop amplitude response is measured using a laser light extinction approach (cf. Fig. 2) [45]. A helium-neon laser beam (632.8 nm wavelength) passes horizontally through the drop and the intensity of the occluded beam is measured using an optical sensor in front of which we place a plate with a 3 mm hole. The overall light intensity I measured by the sensor is proportional to the drop oscillation amplitude. It is noted that the laser used here is not collimated and so some mild beam divergence may exist; however, this should not affect the relationship between the amplitude of drop oscillation and the detector signal, as long as the distances between laser, drop, and sensor are constant, which they are in these experiments. At each excitation frequency, we measure the amplitude and frequency of the drop oscillation by taking the FFT of the time trace. Each experiment yielded a frequency response, a plot of the magnitude of the drop oscillation amplitude against the excitation frequency. The frequency corresponding to the maximum value of this plot is the natural frequency of that particular drop.

Results.—Figure 3 is a plot of the frequency response for a 1.54 mm drop with shear modulus G=75 Pa. The curve shows a single peak at f=121.1 Hz which is the natural frequency for that particular drop. Note the peak exhibits a small bandwidth, indicative of weak viscous effects. The frequency response curves for the other gels similarly exhibit a single peak but at a different frequency. We perform 66 experiments to quantify the dependence of

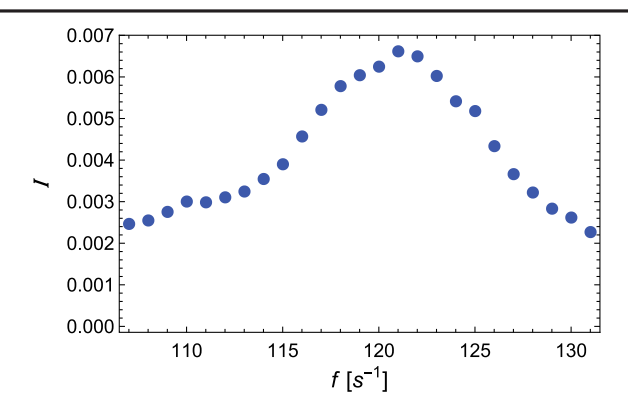


FIG. 3. Frequency response plotting light intensity I against excitation frequency f for an R=1.54 mm drop with shear modulus G=75 Pa yields a resonance frequency of 121.1 Hz.

the natural frequency on G and R. The elastocapillary number $\Sigma \equiv \sigma/RG$ defines the relative importance of surface tension to elastic effects and its value ranges from $\Sigma = 0.22$ –21.07 in our experiments.

Before analyzing our data further, it will be useful to discuss the physics of drop oscillations and the relevant scaling laws in the distinguished limits: elasticity $\Sigma \to 0$ and surface tension $\Sigma \to \infty$. This will be useful in interpreting the crossover between the two limits. The origin of any oscillation is the competition between inertia and a restorative force. For gel drops, both surface tension and elasticity resist deformation and it is natural to view these forces schematically as springs in a simple harmonic oscillator whose normalized spring constant k/m is simply the natural frequency squared $\omega_n^2 = k/m$ of the oscillator. Here the normalization is with respect to the inertia. We are interested in the n=2 shape oscillations observed in our experiments. Unfortunately, no theoretical model of free drop oscillations exists in the literature which couples surface tension and elasticity, although Chakrabarti and Chaudhury [40] propose a model for sessile drops. There are uncoupled models for free drops that incorporate surface tension [1] and elasticity [39,46] separately and we simply state those results. The natural frequency for an inviscid liquid drop held by surface tension is given by

$$\omega_{\sigma}^2 = \frac{8\sigma}{\rho R^3},\tag{2}$$

whereas that of an incompressible elastic globe is

$$\omega_G^2 = C \frac{G}{\rho R^2},\tag{3}$$

with different constants C reported in the literature. For example, a linear elasticity model for the spheroidal modes of oscillation predicts C = 7.1 [39], while a low-order approximate method of the continuum mechanics yields C = 10 in the low-frequency limit [46]. Prestress can also

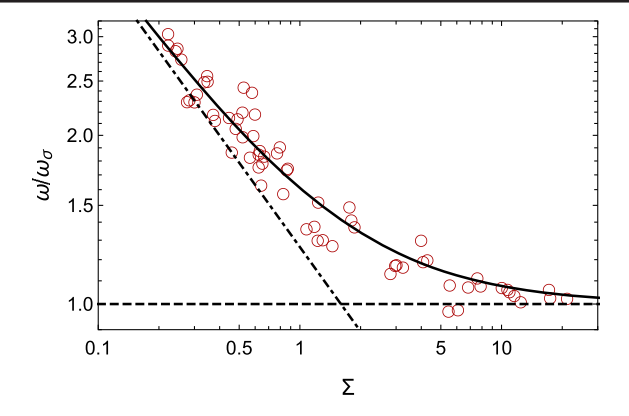


FIG. 4. Scaled angular frequency ω/ω_{σ} against elastocapillary number Σ exhibits a transition between the capillary (dashed line) and elasticity (dot-dashed line) limits. The solid line is the best-fit composite expansion (4).

affect C. Henceforth, we treat C as a fit parameter noting that the scaling law remains unchanged. We expect to recover the appropriate scaling laws, Eqs. (2) and (3), in the distinguished limits, $\Sigma \to \infty$ and $\Sigma \to 0$, respectively. The crossover between these two regimes is determined by setting $\omega_{\sigma}^2 = \omega_G^2$, which yields a critical elastocapillary number $\Sigma_c = C/8$ that separates capillary-dominated $\Sigma > \Sigma_c$ and elasticity-dominated $\Sigma < \Sigma_c$ motions. We are particularly interested in the crossover region where both surface tension and elasticity affect the oscillation dynamics. Using the oscillator perspective, surface tension and elasticity effects can be idealized as springs coupled in parallel and this coupling admits an effective natural frequency for the drop

$$\frac{\omega}{\omega_{\sigma}} = \sqrt{1 + \left(\frac{C}{8}\right)\frac{1}{\Sigma}},\tag{4}$$

where we have scaled the frequency by the capillary frequency (2). This composite expansion yields an explicit dependence of the natural frequency on the elastocapillary number Σ . By construction, Eq. (4) recovers the limiting cases $\Sigma \to \infty$ (2) and $\Sigma \to 0$ (3).

We scale the experimentally observed frequency by the capillary frequency (2), ω/ω_{σ} , and plot our entire dataset against the elastocapillary number Σ in Fig. 4. Our results capture the transition between elasticity-dominated (dot-dashed line) and capillary-dominated (dashed line) regimes and we recover the appropriate scaling laws in the respective limits. We fit our data to the composite dispersion relationship (4) which yields a best-fit parameter value C=12.75 which is slightly larger than that predicted by existing elastic theories C=7.1, C=10 [39,46] but still reasonable. The order of magnitude agreement suggests the composite dispersion relationship (4) reproduces the essential physics and yields a critical elastocapillary number $\Sigma_c=1.59$ using our data.

Discussion.—We have reported the experimental observation of an oscillating gel drop over a range of experimental conditions where elastocapillary effects are important. This is a canonical problem in elastocapillary dynamics and has the potential to impact this emerging field in the same manner in which the analysis of the Rayleigh drop has influenced the field of capillary dynamics, and associated applications, for more than a century. Scaling laws are recovered in the appropriate limits and we show that a proposed relationship for the natural frequency of an elastocapillary drop, that depends upon a nondimensional elastocapillary number, captures the essential physics in the crossover region. Our experimental results yield a precise value of the elastocapillary number which delineates the elastic and capillary wave regimes. These results, as well as an interpretation of the physics, can help improve the aforementioned bioprinting and drop deposition technologies.

Our experimental technique could also be used for material characterization of soft gels. Currently, there are no existing techniques to measure the surface tension of soft gels, despite a large number of those that are suitable for liquids, e.g., Wilhelmy plate, du Nuoy ring, spinning drop, and pendant drop methods, to name a few. These existing methods break down for gels because they either fracture the gel in the case of the du Nuoy ring method or it is impossible to decompose the effect of elasticity from surface tension in the pendant drop method. A recent technique to measure the surface tension of soft gels uses the dispersion relationship of planar elastocapillary waves [47]. There is a rich history of using drop oscillations to determine both surface tension and viscosity in Newtonian liquids and two approaches are generally followed. The first is the finite decay approach whereby a drop shape oscillation is excited and the force is subsequently removed allowing the drop to relax to equilibrium. This approach allows surface tension and viscosity to be extracted from the amplitude time trace [48]. The second approach uses the steady-state frequency response of the drop over a range of excitation frequencies (cf. Fig. 3) to determine the surface tension from the resonance peak and viscosity from the bandwidth [32,49]. The second approach has been extended to surface elasticity and surface dilational viscosity of surfactants on levitated drops [50,51].

Lastly, we note that the dynamics of soft materials are naturally more complex than the statics due to the time scale associated with shape reconfiguration. The situation can become even more complicated for gels with a more complex rheology than the agarose gels we use here due to the additional relaxation time scale, leading to interesting behaviors. This difference is readily seen in classical elastocapillary studies of static [52–54] and dynamic [55–57] wetting ridges with the latter exhibiting complex stick-slip and stick-breaking behaviors. We hope that our study inspires many follow on studies of dynamic elastocapillary phenomena to move this field forward.

J. B. B. acknowledges support from NSF Grant No. CBET-1750208.

- [1] L. Rayleigh, Proc. R. Soc. London **29**, 71 (1879).
- [2] C. Miller and L. Scriven, J. Fluid Mech. 32, 417 (1968).
- [3] A. Prosperetti, J. Mec. 19, 149 (1980).
- [4] J. Tsamopoulos and R. Brown, J. Fluid Mech. 127, 519 (1983).
- [5] S. Ji and M. Guvendiren, Front. Bioeng. Biotechnol. **5**, 23 (2017).
- [6] R. Suntornnond, J. An, and C. K. Chua, Macromol. Mater. Eng. 302, 1600266 (2016).
- [7] M. Gao, L. Li, and Y. Song, J. Mater. Chem. C 5, 2971 (2017).
- [8] M. Rubinstein and R. Colby, Polymer Physics (OUP, Oxford, 2003), ISBN 9780198520597.
- [9] U. Demirci and G. Montesano, Lab Chip 7, 1139 (2007).
- [10] R. W. Style, A. Jagota, C.-Y. Hui, and E. R. Dufresne, Annu. Rev. Condens. Matter Phys. 8, 99 (2017).
- [11] J. Bico, É. Reyssat, and B. Roman, Annu. Rev. Fluid Mech. 50, 629 (2018).
- [12] S. Mora, T. Phou, J.-M. Fromental, and Y. Pomeau, Phys. Rev. Lett. 113, 178301 (2014).
- [13] I. Maimouni, J. Goyon, E. Lac, T. Pringuey, J. Boujlel, X. Chateau, and P. Coussot, Phys. Rev. Lett. 116, 154502 (2016).
- [14] S. Mora, C. Maurini, T. Phou, J.-M. Fromental, B. Audoly, and Y. Pomeau, Phys. Rev. Lett. 111, 114301 (2013).
- [15] M. Adda-Bedia and L. Mahadevan, Proc. R. Soc. A 462, 3233 (2006).
- [16] J. Dervaux and M. B. Amar, Annu. Rev. Condens. Matter Phys. 3, 311 (2012).
- [17] B. Saintyves, O. Dauchot, and E. Bouchaud, Phys. Rev. Lett. 111, 047801 (2013).
- [18] K. E. Daniels, S. Mukhopadhyay, P. J. Houseworth, and R. P. Behringer, Phys. Rev. Lett. 99, 124501 (2007).
- [19] M. Grzelka, J. B. Bostwick, and K. E. Daniels, Soft Matter 13, 2962 (2017).
- [20] V. Bergeron, D. Bonn, J. Y. Martin, and L. Vovelle, Nature (London) 405, 772 (2000).
- [21] D. Bartolo, A. Boudaoud, G. Narcy, and D. Bonn, Phys. Rev. Lett. 99, 174502 (2007).
- [22] M. I. Smith and V. Bertola, Phys. Rev. Lett. 104, 154502 (2010).
- [23] F. Monroy and D. Langevin, Phys. Rev. Lett. **81**, 3167 (1998).
- [24] P. L. Marston and R. E. Apfel, J. Colloid Interface Sci. 68, 280 (1979).
- [25] C.-J. Hsu and R. E. Apfel, J. Colloid Interface Sci. 107, 467 (1985).
- [26] E. H. Trinh and C. J. Hsu, J. Acoust. Soc. Am. 79, 1335 (1986).
- [27] R. H. Temperton, R. J. Hill, and J. S. Sharp, Soft Matter 10, 5375 (2014).
- [28] J. R. Weber, D. S. Hampton, D. R. Merkley, C. A. Rey, M. M. Zatarski, and P. C. Nordine, Rev. Sci. Instrum. 65, 456 (1994).
- [29] J. R. Saylor and B. K. Jones, Phys. Fluids **17**, 031706 (2005).

- [30] B. K. Jones and J. R. Saylor, J. Atmos. Ocean. Technol. 26, 2413 (2009).
- [31] P. H. Steen, C.-T. Chang, and J. B. Bostwick, Proc. Natl. Acad. Sci. U.S.A. **116**, 4849 (2019).
- [32] E. Trinh, A. Zwern, and T. G. Wang, J. Fluid Mech. 115, 453 (1982).
- [33] R. E. Apfel, Y. Tian, J. Jankovsky, T. Shi, X. Chen, R. G. Holt, E. Trinh, A. Croonquist, K. C. Thornton, A. Sacco et al., Phys. Rev. Lett. 78, 1912 (1997).
- [34] J. G. McDaniel and R. G. Holt, Phys. Rev. E 61, R2204 (2000).
- [35] V. A. Hosseinzadeh, C. Brugnara, and R. G. Holt, Sci. Rep. 8, 16794 (2018).
- [36] H. Lamb, Proc. London Math. Soc. s1-13, 189 (1881).
- [37] C. Chree, Trans. Cambridge Philos. Soc. 14, 250 (1889).
- [38] Y. Sato, Geophysical Magazine 31, 15 (1962).
- [39] A. C. Eringen, E. S. Suhubi, and C. Chao, J. Appl. Mech. 45, 229 (1978).
- [40] A. Chakrabarti and M. K. Chaudhury, Extreme Mech. Lett. 1, 47 (2014).
- [41] A. Chakrabarti, Ph.D. thesis, Lehigh University, 2017.
- [42] M. Tokita and K. Hikichi, Phys. Rev. A 35, 4329 (1987).
- [43] S. Mora, T. Phou, J.-M. Fromental, L. M. Pismen, and Y. Pomeau, Phys. Rev. Lett. 105, 214301 (2010).
- [44] E. H. Trinh, Rev. Sci. Instrum. 56, 2059 (1985).

- [45] P. L. Marston and E. H. Trinh, J. Acoust. Soc. Am. 77, S20 (1985).
- [46] S. I. Bastrukov, Phys. Rev. E 49, 3166 (1994).
- [47] X. Shao, J. R. Saylor, and J. B. Bostwick, Soft Matter 14, 7347 (2018).
- [48] J. Kremer, A. Kilzer, and M. Petermann, Rev. Sci. Instrum. 89, 015109 (2018).
- [49] E. Trinh and T. G. Wang, J. Fluid Mech. 122, 315 (1982).
- [50] Y. Tian, R. G. Holt, and R. E. Apfel, Phys. Fluids 7, 2938 (1995).
- [51] Y. Tian, R. G. Holt, and R. E. Apfel, J. Colloid Interface Sci. 187, 1 (1997).
- [52] E. R. Jerison, Y. Xu, L. A. Wilen, and E. R. Dufresne, Phys. Rev. Lett. 106, 186103 (2011).
- [53] R. W. Style, R. Boltyanskiy, Y. Che, J. S. Wettlaufer, L. A. Wilen, and E. R. Dufresne, Phys. Rev. Lett. 110, 066103 (2013).
- [54] J. B. Bostwick, M. Shearer, and K. E. Daniels, Soft Matter 10, 7361 (2014).
- [55] T. Kajiya, A. Daerr, T. Narita, L. Royon, F. Lequeux, and L. Limat, Soft Matter 9, 454 (2013).
- [56] S. Karpitschka, S. Das, M. van Gorcum, H. Perrin, B. Andreotti, and J. H. Snoeijer, Nat. Commun. 6, 7891 (2015).
- [57] S. Park, J. Bostwick, V. De Andrade, and J. Je, Soft Matter 13, 8331 (2017).